Byeongsik Ko
Benson H. Tongue
Andrew Packard
Active Noise Control Laboratory
Department of Mechanical Engineering
University of California at Berkeley
Berkeley, CA 94720

A Method for Determining the Optimal Location of a Distributed Sensor/Actuator

The optimal location problem of distributed sensor/actuator for observation and control of a flexible structure is investigated. Using a property of controllability and observability grammian matrices, this approach employs a nonlinear optimization technique to determine the optimal placement of a distributed sensor/actuator. The effect of unimportant modes that do not strongly affect the structural behavior of a system is minimized and the effect of important modes is maximized. The final objective function is expressed as the combinational form of two different objective functions. This technique is applied to several types of beam support conditions and the corresponding optimal locations are determined. © *1994 John Wiley & Sons, Inc.*

INTRODUCTION

A major avenue for sound generation is through the action of vibrating structural surfaces. One example is the low-frequency interior noise (called boom) that occurs in automobile passenger compartments. This is a particularly complicated problem because the sound comes from the road, engine, and power train excitations transmitted through the structure and into the cabin. The sound is transmitted due to the structural vibration of the surrounding surfaces of the enclosure, and is especially strong when the structural vibration modes and acoustic modes of the enclosure are coupled. This phenomenon occurs between 20 and 60 Hz in most passenger cars. Boom noise has become a critical issue as the automobile body has become lighter in order to save weight, thus leading to increased noise levels.

The coupling effect is a critical problem in automobile design because it so strongly affects booming noise, due to the structural–acoustic coupling of an automotive cabin. There currently exist two methods by which one can control acoustics in an active manner. The first is to inject "antisound" by means of speakers, that is, sound that destructively interferes with the offending noise. The second approach is to use a distributed sensor/actuator and implement a control strategy to control the structural vibrations that affect acoustic modes. If the structural vibration modes can be controlled, the acoustic response will be suppressed.

The control of flexible structure has been studied for several years now. Piezoelectric material was first used to measure the vibration of a mechanical system by Lee and Moon (1990), who along with other researchers (Chiang, and O'Sullivan, 1991) tailored a piezoelectric sensor to measure a single vibration mode. The piezoelectric sensor was designed to be very sensitive to a desired mode while remaining insensitive to the remaining modes. In this way, the sensor filtered out the contribution of the undesired modes. Because each sensor is tailored to detect a single mode, if multiple modes are to be measured, a single sensor is needed for each mode. To mea-

Received September 12, 1993; Revised October 14, 1993

Shock and Vibration, Vol. 1, No. 4, pp. 357–374 (1994)

CCC 1070-9622/94/040357-18

sure a single mode while rejecting the remaining modes, the width of the sensor must be proportional to the second derivative of the desired mode shape. Because it is very difficult to shape the piezoelectric sensor in accordance with this second derivative, an alternative approach is needed. To date, little work has been done to develop a systematic approach for finding the optimal location of sensor/actuators, but much effort has been put into creating a definition of controllability and observability (Arbel, 1981; Hamden and Nayfeh, 1989). Lim (1992) proposed a method for finding optimal sensor and actuator locations. This approach is based on projecting eigenvectors into the intersection subspace of the controllability and observability subspaces of each collocated sensor–actuator pair. Maghami and Joshi (1993) suggested the optimization of a function of the singular values of the Hankel matrix as a criterion for sensor/actuator placement. Each of these methods applies to the case of a discrete actuator and sensor pair.

In addition to the problem of optimal sensor location, it is also necessary to find the optimal location of a distributed actuator. The distributed actuator is well-suited for the control of vibration modes because it is space efficient, light-weight, and requires no external supports. Bailey and Hubbard (1987) first applied a distributed actuator to control the first vibration mode of a clamped-free beam. They demonstrated a drastic change in the decay rate of the impulse response when a distributed actuator is used as an active damper. Crawley and de Luis (1986) experimentally evaluated the effectiveness of using a piezoelectric actuator as a control source.

In this article we consider the design problem of locating a distributed sensor/actuator to maximize performance indices with regard to measurement and control of structural vibrations in a low frequency range. One objective of this work is to find the optimal location of a uniform piezoelectric sensor to sense effectively the specific vibration modes of a flexible structure. The method used is based on the properties of the observability grammian matrix because this matrix represents the degree of observability of a system's modes. A second objective of this work is to find the optimal location of a piezoceramic actuator to control effectively the specific vibration modes of a flexible structure. The method used is based on the properties of the controllability grammian matrix, which represents the degree of controllability of the modes. In this work, the model is assumed to be a linear, second-order dynamic system. Another assumption is that we shall predetermine which are the important vibration modes that must be controlled via optimal feedback control.

CONSTITUTIVE EQUATIONS OF PIEZOELECTRIC MATERIAL

In this section, the governing equations for a piezoelectric material are derived. The constitutive equations for piezoelectric materials can be expressed in terms of the piezoelectric constants that couple the mechanical strain, stress, electric field, and electric displacement based on the IEEE standard on piezoelectricity (1987):

$$\sigma_{ij} = c^{E}_{ijkl}\varepsilon_{kl} - e_{kij}E_k \tag{1}$$

$$D_i = e_{ikl}\varepsilon_{kl} + \epsilon^{\varepsilon}_{ik}E_k \tag{2}$$

where σ_{ij} is the stress tensor, ε_{kl} is the strain tensor, E_k is the electric field, D_i is the electric displacement (or electric flux density, the charge distributed uniformly over a surface), and c_{ijkl}, e_{kij}, and ϵ_{ik} indicate the stiffness matrix, the piezoelectric stress/charge constant matrix, and the piezoelectric permittivity constant of a piezoelectric material. Because the stress and strain matrices σ_{ij} and ε_{kl} are symmetric, the matrix notation can be replaced by vector notation σ_p and ε_{kl}, such that 11, 22, 33, 12, 13, and 23 of the subscripts ij and kl matches to 1, 2, 3, 4, 5, and 6 of the subscripts p and q. Similarly, the stiffness matrix c^{E}_{ijkl} and the piezoelectric stress/charge constant matrix e_{kij} can be expressed in the reduced-order matrix notation c^{E}_{pq} and e_{kp}.

$$\sigma_p = c^{E}_{pq}\varepsilon_q - e_{kp}E_k \tag{3}$$

$$D_i = e_{iq}\varepsilon_q + \epsilon^{\varepsilon}_{ik}E_k. \tag{4}$$

The subscript in σ_p and ε_p denotes the normal stress and strain for $p = 1, 2, 3$ and the shear stress and strain for $p = 4, 5, 6$. The piezoelectric stress/charge matrix of piezoelectric material e_{pq} can be expressed as $e_{pq} = c^{E}_{qs}d_{\mathrm{ps}}$ where d_{ps} represents the piezoelectric strain/charge matrix of the piezoelectric material and is defined as the ratio of the induced strain to the applied field in the stress-free state. As an alternative form, it can also be defined as the ratio of charge per unit area to the applied stress (with no external elec-

tric field). The stiffness matrix c_{pq}^{E} is given by

$$[c_{pq}^{E}] = \begin{bmatrix} \lambda + 2\mu & \lambda & \lambda & 0 & 0 & 0 \\ \lambda & \lambda + 2\mu & \lambda & 0 & 0 & 0 \\ \lambda & \lambda & \lambda + 2\mu & 0 & 0 & 0 \\ 0 & 0 & 0 & \mu & 0 & 0 \\ 0 & 0 & 0 & 0 & \mu & 0 \\ 0 & 0 & 0 & 0 & 0 & \mu \end{bmatrix} \tag{5}$$

where

$$\lambda = \frac{\nu E}{(1 + \nu)(1 - 2\nu)} \quad \text{and} \quad \mu = \frac{E}{2(1 + \nu)}$$

are two Lame's constants. The dielectric permittivity matrix ϵ_{ik}^{e} can be expressed as

$$[\epsilon_{ik}^{e}] = \begin{bmatrix} \epsilon_{11} & 0 & 0 \\ 0 & \epsilon_{22} & 0 \\ 0 & 0 & \epsilon_{33} \end{bmatrix}. \tag{6}$$

For a thin film of a polarized material (taking the z-direction as the poling direction), the piezoelectric strain constant d_{ps} is given by Sessler's work (1981) as

$$d_{ps} = \begin{bmatrix} 0 & 0 & 0 & 0 & d_{15} & 0 \\ 0 & 0 & 0 & d_{15} & 0 & 0 \\ d_{31} & d_{32} & d_{33} & 0 & 0 & 0 \end{bmatrix}. \tag{7}$$

Thus, for linear isotropic materials under plane stress, the governing equations become

$$\begin{pmatrix} \sigma_1 \\ \sigma_2 \\ \sigma_3 \end{pmatrix} = [C] \begin{pmatrix} \varepsilon_1 \\ \varepsilon_2 \\ \varepsilon_3 \end{pmatrix} - [C] \begin{pmatrix} d_{31}E_3 \\ d_{31}E_3 \\ 0 \end{pmatrix} \tag{8}$$

$$D_3 = \epsilon_3 E_3 + d_{31}\sigma_1 + d_{32}\sigma_2 \tag{9}$$

where the stiffness matrix is

$$[C] = \frac{E}{1 - \nu^2} \begin{bmatrix} 1 & \nu & 0 \\ \nu & 1 & 0 \\ 0 & 0 & \dfrac{1 - \nu}{2} \end{bmatrix} \tag{10}$$

and where E is Young's modulus and ν is the Poisson's ratio of the piezoelectric material.

The strains are related to the displacements u, v, and w in x, y, and z directions. The displacement in the x-direction from the undeformed to the deformed neutral axis is u_0. It is assumed that the point C on the neutral axis undergoes a linear displacement u_0 in the x-direction, the line perpendicular to the neutral axis, BD, remains straight and perpendicular to the neutral axis, and the displacement of any point on BD in the x-direction is given by the linear relationship,

$$u = u_0 - z_A\beta = u_0 - z_A \frac{\partial w_0}{\partial x} \tag{11}$$

as shown in Fig. 1.

Generally, the displacement u in the x-direction for any point at a distance z from the neutral axis is given by

$$u = u_0 - z \frac{\partial w_0}{\partial x}. \tag{12}$$

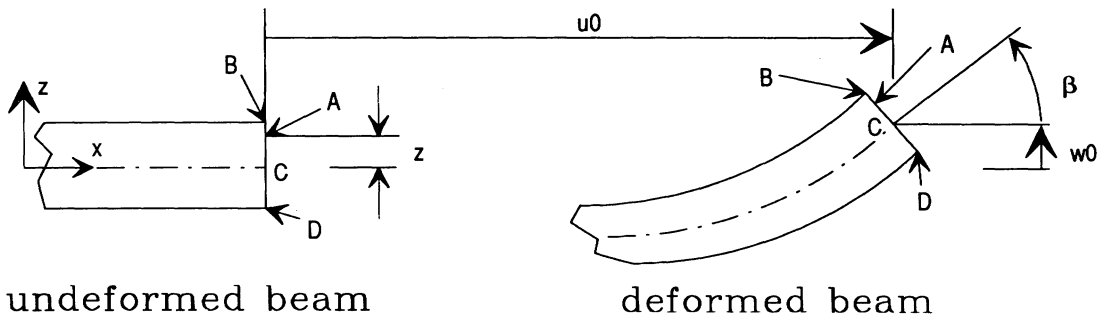

FIGURE 1 Displacement in undeformed coordinate system.

The subscript 0 indicates that the deformation is expressed with respect to the undeformed coordinate system. Similarly v, the displacement in the y-direction for any point at a distance z from the neutral axis, is given by

$$v = v_0 - z\frac{\partial w_0}{\partial y}. \tag{13}$$

From linear elasticity, the strains are as follows:

$$\varepsilon_1 = \frac{\partial u}{\partial x} = \frac{\partial u_0}{\partial x} - z\frac{\partial^2 w_0}{\partial x^2} \tag{14}$$

$$\varepsilon_2 = \frac{\partial v}{\partial y} = \frac{\partial v_0}{\partial y} - z\frac{\partial^2 w_0}{\partial y^2} \tag{15}$$

and

$$\varepsilon_3 = \frac{\partial u}{\partial y} + \frac{\partial v}{\partial x} = \frac{\partial u_0}{\partial y} + \frac{\partial v_0}{\partial x} - z\frac{\partial^2 w_0}{\partial x\,\partial y}. \tag{16}$$

Thus,

$$\begin{pmatrix}\varepsilon_1\\ \varepsilon_2\\ \varepsilon_6\end{pmatrix} = \begin{pmatrix}\dfrac{\partial u_0}{\partial x}\\ \dfrac{\partial v_0}{\partial y}\\ \dfrac{\partial u_0}{\partial y} + \dfrac{\partial v_0}{\partial x}\end{pmatrix} - z\begin{pmatrix}\dfrac{\partial^2 w_0}{\partial x^2}\\ \dfrac{\partial^2 w_0}{\partial y^2}\\ \dfrac{\partial^2 w_0}{\partial x \partial y}\end{pmatrix}. \tag{17}$$

Consider the induced charge due to a mechanical deformation. From Gauss' law, it is known that the charge enclosed by a surface S is

$$q = \int_S \vec{D} \cdot d\vec{\sigma} \tag{18}$$

where $\vec{D}$ is the electric displacement vector and $d\vec{\sigma}$ is the differential area vector normal to S. Because charge is built up on the surface of a piezoelectric lamina when it experiences mechanical strain, we can use an equivalent circuit model for a piezoelectric sensor, as shown in Fig. 2, to relate the closed-circuit charge signal measured from the surface electrode to the strain in the beam.

By substituting Eq. (8) and Eq. (17) into Eq. (9), D_3, the electrical displacement in the z-direction can be derived:

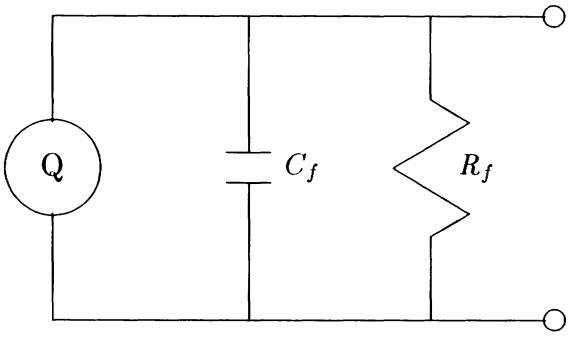

Equivalent circuit for piezo sensor

FIGURE 2 Equivalent circuit of piezoelectric sensor.

$$\begin{aligned} D_3 &= \left[\epsilon_{33} - \frac{E}{1-\nu^2}(d_{31}^2 + d_{32}^2 + 2\nu d_{31}d_{32})\right] E_3 \\ &\quad + \frac{E}{1-\nu^2}(d_{31} + \nu d_{32})\varepsilon_1 \\ &\quad + \frac{E}{1-\nu^2}(d_{32} + \nu d_{31})\varepsilon_2 \\ &= \epsilon_{33}^M E_3 + e_{31}\varepsilon_1 + e_{32}\varepsilon_2 \end{aligned} \tag{19}$$

where

$$\epsilon_{33}^M = \epsilon_{33} - \frac{E}{1-\nu^2}(d_{31}^2 + d_{32}^2 + 2\nu d_{31}d_{32}) \quad \text{and}$$

$$\begin{pmatrix}\varepsilon_{31}\\ \varepsilon_{32}\end{pmatrix} = \frac{E}{1-\nu^2}\begin{bmatrix}1 & \nu\\ \nu & 1\end{bmatrix}\begin{pmatrix}d_{31}\\ d_{32}\end{pmatrix}.$$

The total induced charge q on the piezoelectric surfaces can be obtained by integrating the electric displacement D_3 over the domain covered by two sides of the piezoelectric sensor

$$\begin{aligned} q &= \int\int_{S_0} D_3\, dx\, dy \\ &= \epsilon_{33}^M E_3 S_0 + e_{31}\int\int_{S_0}\left(\frac{\partial u_0}{\partial x} - z\frac{\partial^2 w_0}{\partial x^2}\right) dx\, dy \\ &\quad + e_{32}\int\int_{S_0}\left(\frac{\partial v_0}{\partial y} - z\frac{\partial^2 w_0}{\partial y^2}\right) dx\, dy. \end{aligned} \tag{20}$$

Because we are interested in the charge signal in a dynamic range, we can set $E_3 = 0$. Then the charge signal in a closed circuit induced by the piezoelectric material can be expressed by

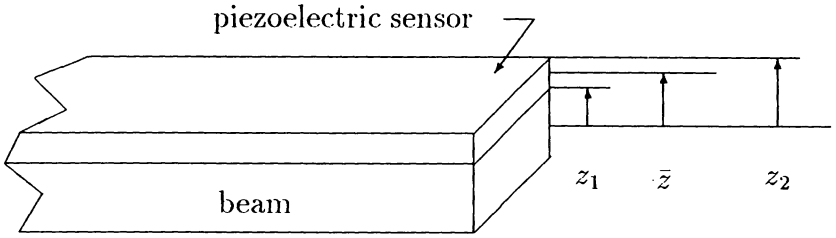

FIGURE 3 Coordinates in beam-distributed sensor system.

$$q = e_{31} \int\int_{S_0} \left(\frac{\partial u_0}{\partial x} - z\frac{\partial^2 w_0}{\partial x^2}\right) dx\, dy + e_{32} \int\int_{S_0} \left(\frac{\partial v_0}{\partial y} - z\frac{\partial^2 w_0}{\partial y^2}\right) dx\, dy = e_{31} \int\int_{S_0} \frac{\partial u_0}{\partial x} dx\, dy + e_{32} \int\int_{S_0} \frac{\partial^2 v_0}{\partial y} dx\, dy - \bar{z}\left(e_{31} \int\int_{S_0} \frac{\partial^2 w_0}{\partial x^2} dx\, dy + e_{32} \int\int_{S_0} \frac{\partial^2 w_0}{\partial y^2} dx\, dy\right) \quad (21)$$

where $\bar{z}$ is the distance between the center of piezoelectric sensor and neutral axis of the beam-sensor system (Fig. 3).

From the definition of the neutral axis (the axis with invariant length under bending), it is seen that $u_0 = v_0 = 0$. The induced charge signal is given by

$$q = -\bar{z}\left(e_{31} \int\int_{S_0} \frac{\partial^2 w_0}{\partial x^2} dx\, dy + e_{32} \int\int_{S_0} \frac{\partial^2 w_0}{\partial y^2} dx\, dy\right). \quad (22)$$

For a beam,

$$q = -\bar{z}e_{31} \int\int_{S_0} \frac{\partial^2 w_0}{\partial x^2} dx\, dy = -\bar{z}e_{31} b_{pe} \int_{x_{1s}}^{x_{2s}} \frac{\partial^2 w_0}{\partial x^2} dx \quad (23)$$

where b_{pe} is the width of the piezoelectric sensor.

GOVERNING EQUATIONS FOR A DISTRIBUTED ACTUATOR

A piezoceramic actuator elongates or contracts as the polarity changes when it is exposed to an alternating voltage. A voltage applied across the piezoceramic actuator induces an interface stress and strain between the piezoelectric actuator and the underlying structure. Assuming a stress-free state initially, the induced strain of piezoceramic actuator under an applied voltage V will be defined by

$$\varepsilon_p = \frac{d_{31}}{t_a} V \quad (24)$$

where d_{31} is the ratio of the induced strain to the applied field in the stress-free state, and t_a is the thickness of the piezoceramic actuator. The stress distribution over cross section is discontinuous at the interface between the piezoceramic and the beam. Because the piezoceramic actuator is attached on one side of the beam, the stress distribution across the beam is not symmetric about the centerline of the beam. Therefore the stress distribution across the beam can be expressed as a combination of pure bending stress and pure extensional stress.

The strain distribution across the beam, as shown in Fig. 4, is

$$\varepsilon = \kappa z + \varepsilon_0 \quad (25)$$

where ε_0 is the extensional strain and κ is the curvature of the beam-distributed actuator system.

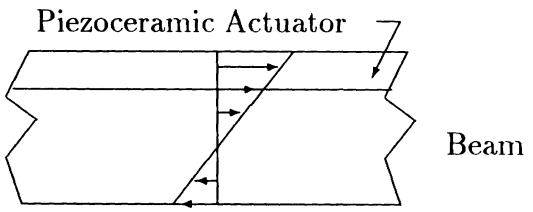

FIGURE 4 Strain distribution in beam-distributed actuator system.

The stress distribution across the beam, as shown in Fig. 5, can be expressed by

$$\sigma_b = E_b(\kappa z + \varepsilon_0) \tag{26}$$

where E_b is the Young's modulus of the beam. Similarly, the stress distribution across the distributed actuator is a combination of pure bending stress, pure extensional stress, and the induced stress by the piezoceramic actuator under an applied voltage V.

$$\sigma_p = E_p(\kappa z + \varepsilon_0 - \varepsilon_p) \tag{27}$$

where E_p is the Young's modulus of the distributed actuator. The frequency range under consideration in the vibration control area is much lower in comparison to the thickness and length resonance frequencies of the distributed actuator, which are typically over 20 kHz. Therefore, its effect can also be neglected in the dynamic behavior of composite structure. Requiring the extensional force and bending moment across the combined system to be in equilibrium, gives:

$$\int_{-h/2}^{h/2} \sigma_b \, dz + \int_{h/2}^{h/2+t_a} \sigma_p \, dz = 0 \tag{28}$$

and

$$\int_{-h/2}^{h/2} \sigma_b z \, dz + \int_{h/2}^{h/2+t_a} \sigma_p z \, dz = 0. \tag{29}$$

From Eq. (28)

$$E_b\varepsilon_0 h + E_p(\varepsilon_0 - \varepsilon_p)t + \frac{1}{2}\kappa E_p t(h + t) = 0. \tag{30}$$

and from Eq. (29)

$$\kappa\left(\frac{1}{12}E_b h^3 + \frac{1}{3}E_p\left[t^3 + \frac{3}{2}ht^2 + \frac{3}{4}h^2 t\right]\right) + \frac{1}{2}E_p\varepsilon_o t(h + t) = \frac{1}{2}E_p\varepsilon_p t(h + t). \tag{31}$$

Introducing two nondimensional numbers, $\beta = E_p/E_b$ and $k = t/h$, Eq. (30) and Eq. (31) can be expressed as

$$(1 + \beta k)\varepsilon_0 + \frac{1}{2}\kappa h\beta k(1 + k) = \beta k\varepsilon_p \tag{32}$$

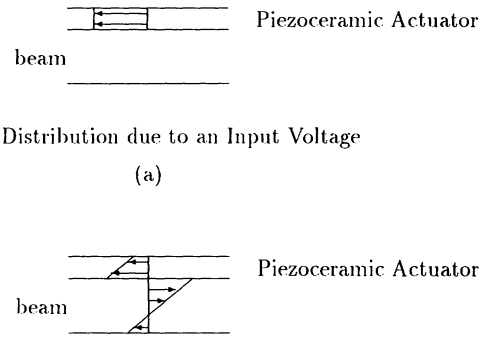

FIGURE 5 Stress distribution in beam-distributed actuator system.

$$\kappa h\left[\frac{1}{12} + \frac{1}{3}\left(k^3 + \frac{3}{2}k^2 + \frac{3}{4}k\right)\right] + \frac{1}{2}\beta k(1 + k)\varepsilon_0 = \frac{1}{2}\beta k(1 + k)\varepsilon_p. \tag{33}$$

From Eq. (32) and Eq. (33) κh and ε_0 can be obtained as follows:

$$\kappa h = K_1\varepsilon_p \tag{34}$$

$$\varepsilon_0 = K_2\varepsilon_p \tag{35}$$

where the coefficients K_1 and K_2 are

$$K_1 = \frac{6(\beta k + \beta k^2)}{1 + 4\beta k + 6\beta k^2 + 4\beta k^3 + \beta^2 k^4} \tag{36}$$

$$K_2 = \frac{\beta k + \beta^2 k^4}{1 + 4\beta k + 6\beta k^2 + 4\beta k^3 + \beta^2 k^4}. \tag{37}$$

The induced bending moment can be obtained by integrating σ_b over the cross section of the beam. The extensional strain component ε_0 does not contribute to the bending moment. The line moment acting on an edge of the actuator is

$$m_x = \int_{h/2}^{-h/2} \sigma_b z \, dz = C_0\varepsilon_{pe}\frac{b_{pa}}{W_b} = \bar{C}V\frac{b_{pa}}{W_b} \tag{38}$$

where C_0 and $\bar{C}$ are constants, which depend on the properties of the piezoceramic actuator and beam, σ_b is the bending stress in the beam, b_{pa} is the width of the piezoceramic actuator, and W_b is the width of the beam. By oscillating the voltage applied to the actuator, the induced line moment m_c will oscillate at the same frequency. The

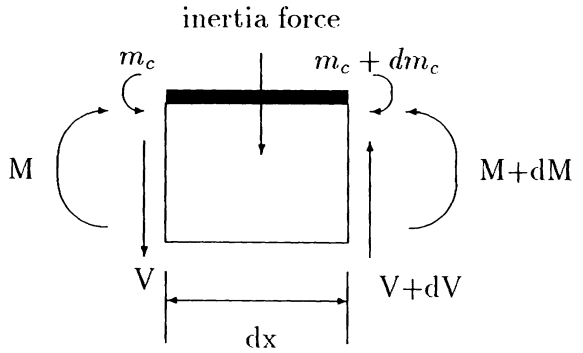

FIGURE 6 Free-body diagram of an infinitesimal mass.

equation of motion of the beam can be written in terms of the internal bending moment M and the actuator-induced moment m_c (Fig. 6):

$$\frac{\partial^2(M - m_c)}{\partial x^2} + m'\ddot{w} = 0 \tag{39}$$

where m' is the mass per unit length.

The internal bending moment M can also be expressed in terms of the displacements w as

$$\frac{\partial^2 M}{\partial x^2} = EI\frac{\partial^4 M}{\partial x^4}. \tag{40}$$

In general, moments M and m_c acting on a structure can be expressed as dipole forces with magnitudes $M\delta'(x - x_0)$ and $m\delta'(x - x_0)$, where x_0 is the location of the moment. Thus applying a voltage to the piezoelectric actuator results in distributed line moments acting on the beam along the boundaries of the piezoceramic actuator.

MATHEMATICAL MODELING OF BEAM WITH A DISTRIBUTED SENSOR/ACTUATOR

The mathematical modeling of clamped-free beams, simply supported beams, and clamped beams are considered. A piezoelectric film is attached to one side of the beam as a sensor (Fig. 7) and a piezoceramic plate is bonded to the other side of the beam as an actuator (Fig. 8). The equation of motion for a beam can be represented as follows:

$$EI\frac{\partial^4 w}{\partial x^4} + m'\ddot{w} = \frac{\partial^2 m_c}{\partial x^2} \tag{41}$$

where m_c is a line moment due to a control input and m' is the mass per unit length of the beam. Assuming that the width of the beam and that of the distributed actuator are the same, the moment m_c due to a distributed actuator can be expressed as

$$m_c = \bar{C}V(\langle x - x_{1a}\rangle^0 - \langle x - x_{2a}\rangle^0) \tag{42}$$

where x_{1a} and x_{2a} are two end points of the distributed actuator. The function $\langle x - x_0\rangle^0$ denotes the unit step function at $x = x_0$ and the subscript c indicates the control input. Using the modal representation

$$w(x, t) = \sum_{n=1}^{\infty} \eta_n(t)\phi_n(x)$$

the partial differential equation can be transformed to

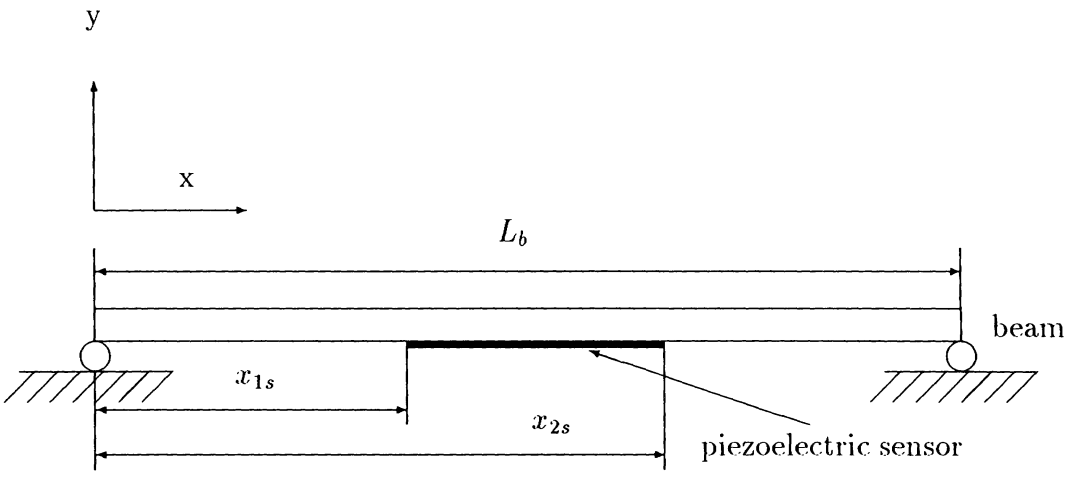

FIGURE 7 Beam-distributed sensor system.

$$EI \sum_n \eta_n \frac{\partial^4 \phi_n}{\partial x^4} + m' \sum_n \phi_n \ddot{\eta}_n = \frac{\partial^2 m_c}{\partial x^2}. \quad (43)$$

The right-hand side can be represented as follows:

$$\begin{aligned} \frac{\partial^2 m_c}{\partial x^2} &= \bar{C}V(\langle x - x_{1a}\rangle^{-2} - \langle x - x_{2a}\rangle^{-2}) \\ &= \bar{C}V[\delta'(x - x_{1a}) - \delta'(x - x_{1a})]. \end{aligned} \quad (44)$$

Multiplying by $\phi_m(x)$, integrating over the entire length of the beam, and using orthogonality leads to

$$m'\ddot{\eta}_m + EI\left(\frac{\lambda_m}{l}\right)^4 \eta_m = b_m u(t) \qquad m = 1, 2, 3, \ldots \quad (45)$$

where $u(t)$ is applied control input V. The representation of $b_m u(t)$ is defined by

$$b_m u(t) = \int_0^l \phi_m \frac{\partial^2 m_c}{\partial x^2} = \bar{C}V\left(\frac{d\phi_m}{dx}\bigg|_{x=x_{2a}} - \frac{d\phi_m}{dx}\bigg|_{x=x_{1a}}\right). \quad (46)$$

Next, the system equation of the beam can be expressed in a state-space form as

$$\dot{x} = Ax + Bu \quad (47)$$

where

$$x(t) = \begin{bmatrix} \eta_1 \\ \eta_2 \\ \cdots \\ \eta_N \\ \dot{\eta}_1 \\ \dot{\eta}_2 \\ \cdots \\ \dot{\eta}_N \end{bmatrix}.$$

The A and B matrices are defined as follows:

$$A = \begin{bmatrix} 0 & I \\ -\Omega^2 & -2\zeta\Omega \end{bmatrix}_{2N\times 2N} \quad (48)$$

$$B = \begin{bmatrix} 0 \\ \mathbf{b} \end{bmatrix}_{2N\times 1} \quad (49)$$

where ζ and Ω are diagonal matrices of modal damping factors and the corresponding natural frequencies.

Because a piezoceramic plate induces a mechanical strain when it is charged, it can be used as a vibration actuator. Assuming that a piezoceramic actuator runs from $x = x_{1a}$ to $x = x_{2a}$ when it is attached to the beam, the effective line moment b_m to the mth eigenmode of the beam due to the unit input voltage can be expressed as follows:

$$b_m = \frac{T_m}{m' A_m^2} \quad (50)$$

where T_m is given by

$$T_m = \bar{C}\left(\frac{d\phi_m}{dx}\bigg|_{x=x_{2a}} - \frac{d\phi_m}{dx}\bigg|_{x=x_{1a}}\right).$$

Then the matrix B is defined as

$$B(x_{1a}, x_{2a}) = [0 \quad 0 \cdots 0 \quad b_1 \quad b_2 \cdots b_N]^T_{(2N)\times 1}. \quad (51)$$

Note that the matrix B is a function of the position at two ends of the piezoceramic array.

The piezoelectric film generates an electric charge when it is deformed; therefore the piezoelectric film attached to the vibrating structure can be used as a vibration sensor. Assuming that a piezoelectric sensor runs from $x = x_{1s}$ to $x = x_{2s}$, the induced charge signal $y(t)$ due to the modal deflections ϕ_m, $1 \le m \le N$, can be expressed as follows:

$$y(t) = -z_0 e_{31}^0 b_p \sum_{m=1}^N \eta_m(t) \int_{x_{1s}}^{x_{2s}} \frac{d^2\phi_m}{dx^2} \quad (52)$$

$$= -z_0 e_{31}^0 b_p \sum_{m=1}^N \left(\frac{d\phi_m}{dx}\bigg|_{x=x_{2s}} - \frac{d\phi_m}{dx}\bigg|_{x=x_{1s}}\right) \eta_m(t) \quad (53)$$

$$= \sum_{m=1}^N K_{qm}\eta_m(t) \quad (54)$$

where z_0 is the distance from the neutral axis of the beam to the centerline of the piezoelectric film, coefficient K_{qm} is defined as

$$K_{qm} = -z_0 e_{31}^0 b_p \left(\frac{d\phi_m}{dx}\bigg|_{x=x_{2s}} - \frac{d\phi_m}{dx}\bigg|_{x=x_{1s}}\right)$$

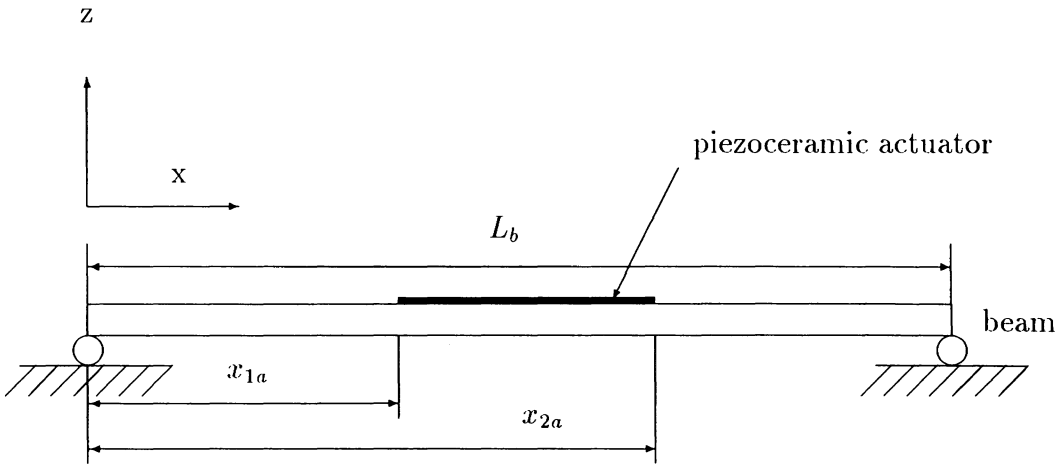

FIGURE 8 Beam-distributed actuator system.

and e_{31}^0 is a piezoelectric stress/charge constant. The matrix C can then be constructed as the row vector:

$$C(x_{1s}, x_{2s}) = [K_{q1} \quad K_{q2} \cdots K_{qN} \quad 0 \quad 0 \cdots 0]_{1\times(2N)}. \tag{55}$$

Note that matrix C is a function of the position of the two ends of the piezoelectric film.

OBSERVABILITY AND CONTROLLABILITY GRAMMIAN MATRICES

Observability

The state-space representation of a constant coefficient, linear system is given as follows:

$$\begin{aligned} \dot{x} &= Ax + Bu \\ y &= Cx + Du. \end{aligned} \tag{56}$$

The state $x(t)$ can be obtained from the given initial state $x(t_0)$ through the state transition matrix:

$$x(t) = \Phi(t, t_0)x(t_0) + \int_{t_0}^{t} \Phi(t, \tau)Bu(\tau)\, d\tau \tag{57}$$

where the transition matrix $\Phi(t, t_0) = e^{A(t-t_0)}$. The sensing output from a uniform piezoelectric sensor $y(t)$ is given by

$$y(t) = C\Phi(t, t_0)x(t_0) + \int_{t_0}^{t} C\Phi(t, \tau)Bu(\tau)\, d\tau. \tag{58}$$

Because the input $u(t)$ is assumed to be known, we can assume $u(t) = 0$ without loss of generality, yielding

$$y(t) = C\Phi(t, t_0)x(t_0). \tag{59}$$

If the columns of $C\Phi(t, t_0)$ are linearly independent over $[t_0, t_f]$, then

$$[C\Phi(t, t_0)x(t_0)]^T y(t) = [C\Phi(t, t_0)x(t_0)]^T C\Phi(t, t_0)x(t_0) \tag{60}$$

$$\int_{t_0}^{t_f} \Phi(t, t_0)^T C^T y(t)\, dt = x(t_0) \int_{t_0}^{t_f} \Phi(t, t_0)^T C^T C\Phi(t, t_0)\, dt \tag{61}$$

where $\int_{t_0}^{t_f} \Phi(t, t_0)^T C^T C\Phi(t, t_0)\, dt$ is the observability grammian matrix $W^o(t_f, t_0)$.

From Eq. (61), the initial state $x(t_0)$ can be expressed in terms of the observability grammian matrix $W^o(t_f, t_0)$ and the measured signal $y(t)$.

$$x(t_0) = W^o(t_f, t_0)^{-1} \int_{t_0}^{t_f} \Phi(t, t_0)^T C^T y(t)\, dt. \tag{62}$$

After obtaining $x(t_0)$ and evaluating Eq. (57), the state trajectory $x(t)$ over $[t_0, t_f]$ can be observed. It is seen that the state $x(t)$, $t \in [t_0, t_f]$, explicitly depends on both $W^o(t_f, t_0)$ and the measured signal $y(t)$ based on Eqs. (62) and (57). Because the model is asymptotically stable for all linear damped flexible structures, the equilibrium solution W_∞^o can be obtained from the following equation

$$W_\infty^o \equiv \lim_{t_f \to \infty} W^o(t_f, t_0)$$

$$= \int_{t_0}^{\infty} \Phi(t, t_0)^T C^T C \Phi(t, t_0)\, dt. \quad (63)$$

W_∞^o satisfies the Lyapunov equation

$$W_\infty^o A + A^T W_\infty^o = -C^T C. \quad (64)$$

If a knowledge of some of the modes of the structure are not required because they do not strongly affect the system's structural vibration or are not strongly coupled to the acoustic field, we need not consider those modes. If their associated frequencies are between the natural frequencies of modes that **do** strongly couple, it would be desirable for the sensor to ignore them and only respond to those modes that couple with the acoustics. Let us separate the problem into two distinct subsystems. Subsystem 1 is composed of the important modes whose grammian matrix eigenvalues must be increased (thus magnifying their effect on the sensor) and subsystem 2 consists of the unimportant modes whose grammian matrix eigenvalues must be decreased (thus minimizing their contribution).

Subsystem 1:

$$\dot{x}_1 = A_1 x_1 \quad (65)$$

$$y_1 = C_1 x_1. \quad (66)$$

Subsystem 2:

$$\dot{x}_2 = A_2 x_2 \quad (67)$$

$$y_2 = C_2 x_2. \quad (68)$$

The observability grammian matrices $W_{1\infty}^o$ and $W_{2\infty}^o$ of these systems satisfy the following Lyapunov equations

$$W_{1\infty}^o A_1 + A_1^T W_{1\infty}^o = -C_1^T C_1 \quad (69)$$

$$W_{2\infty}^o A_2 + A_2^T W_{2\infty}^o = -C_2^T C_2 \quad (70)$$

Because the observability grammian matrix indicates the degree of the observability of the modes, it is proposed that the minimum eigenvalue of $W_{1\infty}^o$ be maximized to increase the degree of observability of important modes. In a similar manner, we require that the maximum eigenvalue of $W_{2\infty}^o$ be minimized in order to decrease the degree of observability of the unimportant modes. Mathematically, these conditions can be expressed as follows:

Subsystem 1:

$$\max_{0 \le x_{1s} < L_b, x_{1s} < x_{2s} \le L_b} \min_i \lambda_i(W_{1\infty}^o)$$

$$= \min_{0 \le x_{1s} < L_b, x_{1s} < x_{2s} \le L_b} [-\min_i \lambda_i(W_{1\infty}^o)]. \quad (71)$$

Subsystem 2:

$$\min_{0 \le x_{1s} < L_b, x_{1s} < x_{2s} \le L_b} \max_j \lambda_j(W_{2\infty}^o). \quad (72)$$

The final optimization problem is to determine x_{1s} and x_{2s} in order to minimize the global performance index J^o. The performance index J^o is the sum of two performance indices, J_1^o and J_2^o, defined by

$$J_1^o = -\min_i \lambda_i(W_{1\infty}^o) \quad (73)$$

$$J_2^o = -\min_j \lambda_j(W_{2\infty}^o). \quad (74)$$

Thus

$$J^o = J_1^o + J_2^o = (-\min_i \lambda_i(W_{1\infty}^o)) + \max_j \lambda_j(W_{2\infty}^o). \quad (75)$$

Controllability

The control input will be chosen so that after some finite time the state must be zero. Moreover, the control energy applied to the control actuator must be minimized. The state $x(t)$ can be obtained from the given initial state $x(t_0)$,

$$x(t) = \Phi(t, t_0)x(t_0) + \int_{t_0}^{t} \Phi(t, \tau)Bu(\tau)\, d\tau. \quad (76)$$

The controllability grammian matrix $W^c(t_f, t_0)$ is defined as

$$W^c(t_f, t_0) = \int_{t_0}^{t_f} \Phi(t, t_0)^T B B^T \Phi(t, t_0)\, dt. \quad (77)$$

The measure of controllability to be used for finding the optimal placement of the distributed actuator can be defined by

$$J = \max_x \min_i \lambda_i[W^c(t_f, t_0)]. \quad (78)$$

Because the model is asymptotically stable for all linear damping flexible structures, the equilibrium solution W_∞^c can be obtained from the Lyapunov equation

$$W_\infty^c \equiv \lim_{t_f \to \infty} W^c(t_f, t_0) = \int_{t_0}^{\infty} \Phi(t, t_0)^T BB^T \Phi(t, t_0)\, dt. \tag{79}$$

W_∞^c satisfies the following Lyapunov equation

$$AW_\infty^c + W_\infty^c A^T = -BB^T. \tag{80}$$

The remaining derivation exactly parallels that of the previous section so we shall simply present the results. The final optimization problem is to design x_{1a} and x_{2a} to minimize the global performance index J^c. The performance index J is a combination of two performance indices J_1^c and J_2^c defined by

$$J_1^c = -\min_i \lambda_i(W_{1\infty}^c) \tag{81}$$

$$J_2^c = \max_j \lambda_j(W_{2\infty}^c). \tag{82}$$

The global performance index J^c that must be minimized over the domain composed of the design variables x_{1a} and x_{2a} is defined by

$$J^o = J_1^c + J_2^c = [-\min_i \lambda_i(W_{1\infty}^c)] + \max_j \lambda_j(W_{2\infty}^c). \tag{83}$$

OPTIMIZATION FOR OBSERVABILITY AND CONTROLLABILITY GRAMMIAN MATRICES

The observability grammian matrix $W_{1\infty}^o$ represents the degree of observability of the modes that must be controlled and the controllability grammian matrix $W_{1\infty}^c$ indicates the degree of controllability of the modes. The minimal eigenvalue of the observability grammian matrix $W_{1\infty}^o$ must be made as large as possible to observe the important modes well and the maximum eigenvalue of a different observability grammian matrix $W_{2\infty}^o$ must be made as small as possible to not detect the unimportant modes. In the case of the controllability grammian matrix the minimal eigenvalue of $W_{1\infty}^c$ should be large to control the important mode well and the maximum eigenvalue of $W_{2\infty}^c$ should be small, so as to not excite the unimportant modes. Thus the final optimization problem for the observability grammian matrix can be expressed as follows:

$$\min_{o \le x_{1s} < L_b, x_{1s} < x_{2s} \le L_b} J^o. \tag{84}$$

The important modes must be chosen before proceeding with the optimization algorithm to determine the optimal location of the distributed sensor.

The numerical procedure for obtaining the optimal locations of the distributed piezoelectric sensor is as follows

Step 1: Guess x_{1s} and x_{2s}, the locations of the two end points of the piezoelectric sensor.

Step 2: Compute the matrices $C_1(x_{1s}, x_{2s})$ and $C_2(x_{1s}, x_{2s})$ functions of x_{1s} and x_{2s}, in $y = Cx$.

Step 3: Solve the Lyapunov equations corresponding to the unimportant modes and the important modes,

$$W_{1\infty}^o A_1 + A_1^T W_{1\infty}^o = -C_1^T C_1$$

$$W_{2\infty}^o A_2 + A_2^T W_{2\infty}^o = -C_2^T C_2$$

to obtain $W_{1\infty}^o$ and $W_{2\infty}^o$.

Step 4: Check the minimum eigenvalue of $W_{1\infty}^o$

Step 5: Check the maximum eigenvalue of $W_{2\infty}^o$

Step 6: If the optimum condition is satisfied, stop. If not, change the positions and go to the 2nd step.

The flow chart for the optimization corresponding to observability grammian matrix is given in Fig. 9.

The numerical procedure for obtaining the optimal locations for the distributed actuator is very similar to that of finding the optimal location for the distributed sensor. The flow chart for the optimization corresponding to the controllability grammian matrix is given in Fig. 10.

SIMULATION: CLAMPED-FREE, SIMPLY SUPPORTED, AND CLAMPED-CLAMPED BEAM

The beam used in this example has the following properties: length: L_b = 0.381 m; width: b = 0.0381 m; thickness; t_b = 3.175 e-3 m; density: ρ_b = 2,700 kg/m^3, Young's modulus: E_b = 60 Gpa. The properties of the piezoelectric sensor are as follows: width: b_p = 0.01 m; thickness: t_p = 110e-6 m; piezoelectric strain/charge constant: d_{31} = 23e-12 m/V; Young's modulus: E_p = 2 Gpa;

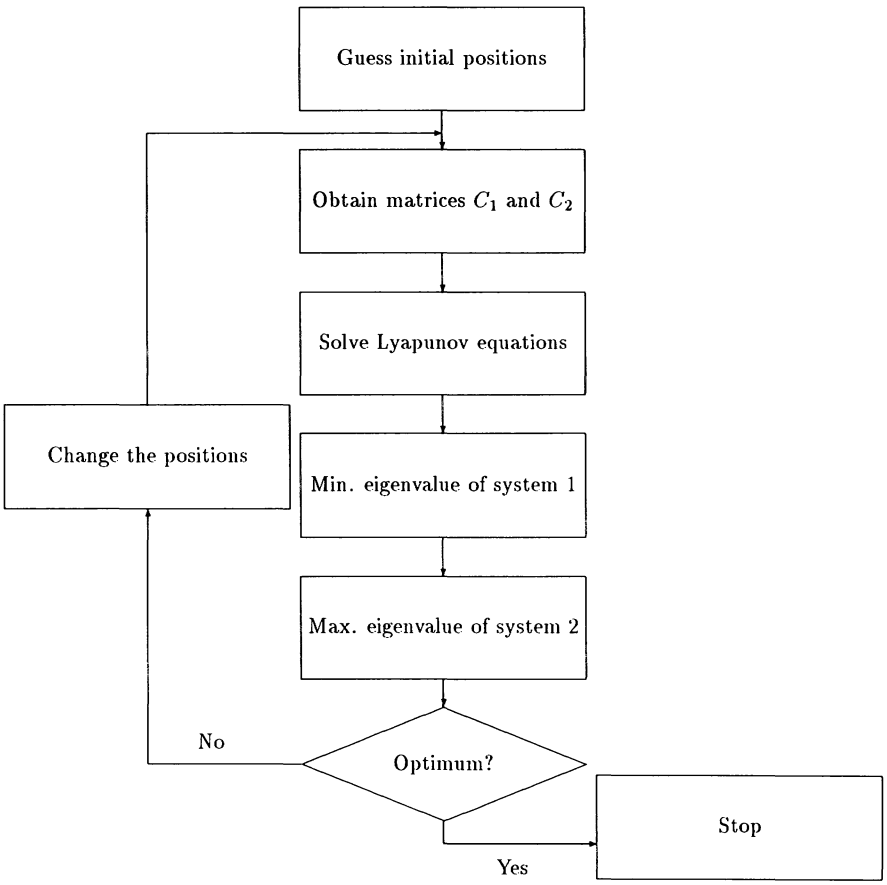

FIGURE 9 Flow chart for optimization in case of a distributed sensor.

Poisson's ratio: $\nu_p = 0.3$; piezoelectric stress/charge constants: e_{31}^0 and e_{32}^0.

$$\begin{pmatrix} e_{31}^0 \\ e_{32}^0 \end{pmatrix} = \begin{bmatrix} \dfrac{E_p}{1-\nu_p^2} & \dfrac{\nu_p E_p}{1-\nu_p^2} \\ \dfrac{\nu_p E_p}{1-\nu_p^2} & \dfrac{E_p}{1-\nu_p^2} \end{bmatrix} \begin{pmatrix} d_{31} \\ d_{32} \end{pmatrix}.$$

The eigenfunctions of a simply supported beam are given as follows:

$$\phi_m(x) = \sqrt{2} \sin\left(\frac{m\pi x}{l_b}\right). \tag{85}$$

The eigenfunctions of a clamped-free beam are

$$\phi_m(x) = \cosh(\beta_m x) - \cos(\beta_m x) - \alpha_m[\sinh(\beta_m x) - \sin(\beta_m x)] \tag{86}$$

$$\alpha_m = \frac{\cosh(\beta_m L_b) + \cos(\beta_m L_b)}{\sinh(\beta_m L_b) + \sin(\beta_m x)} \tag{87}$$

$$\cos(\beta_m L_b)\cosh(\beta_m L_b) = -1. \tag{88}$$

The eigenfunctions of a clamped-clamped beam are

$$\phi_m(x) = \cosh(\beta_m x) - \cos(\beta_m x) - \alpha_m[\sinh(\beta_m x) - \sin(\beta_m x)] \tag{89}$$

$$\alpha_m = \frac{\cosh(\beta_m L_b) - \cos(\beta_m L_b)}{\sinh(\beta_m L_b) - \sin(\beta_m x)} \tag{90}$$

$$\cos(\beta_m L_b)\cosh(\beta_m L_b) = 1. \tag{91}$$

The optimization is performed using the Optimization ToolBox in Matlab (MathWorks, 1991).

OPTIMAL LOCATION OF DISTRIBUTED SENSOR

Table 1 shows the results from the optimization procedure to find the optimal location of a piezoelectric sensor for the cases of a clamped-free, simply supported, and clamped-clamped beam. In the first column, the number in parentheses represents the highest vibration mode that is as-

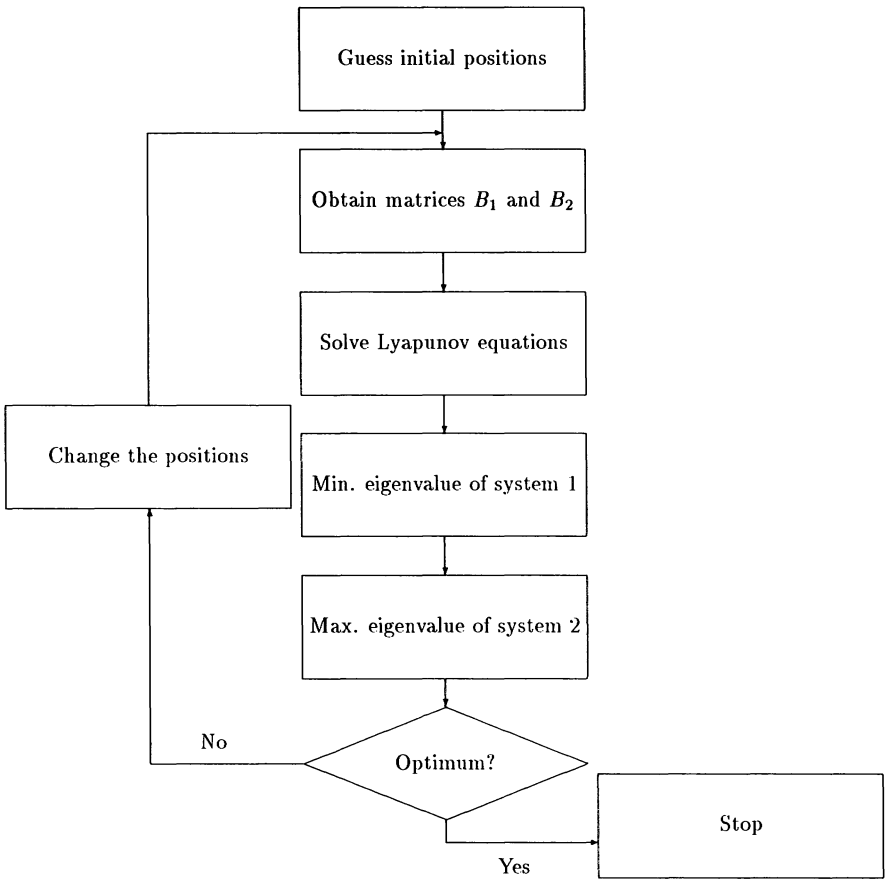

FIGURE 10 Flow chart for optimization in case of a distributed actuator.

sumed to be present in the system. The remaining numbers in the first column correspond to those modes whose contribution to the vibration of the system is assumed to be important. The numbers in parentheses in the second through fourth columns denote the normalized sensor positions, x_{1s}/L_b and x_{2s}/L_b, corresponding to a clamped-free, simply supported, and clamped-clamped beam. The method through which the sensors observe the modes is by measuring the slope at given points. Thus an optimal sensor position occurs when the difference between the

Table 1. Normalized Optimal Locations of a Piezoelectric Sensor

Modes	Clamped-Free Beam	Simply Supported Beam	Clamped-Clamped Beam
1 (2)	(0,0.47082)	(0,1)	(0.22415,0.77585)
1 (3)	N/A	(0.16667,0.8333)	(0.20774,0.79226)
1, 2 (3)	(0.18342,0.76865)	(0.08334,0.58333) or (0.41667,0.91667)	(0.16208,0.53957)
1, 3 (3)	(0.0505,0.4025)	(0,1)	(0.35008,0.64992)
1, 2, 3 (3)	(0.49645,1)	(0,0.3333) or (0.6667,1)	(0.13020,0.41322) or (0.58678,0.86980)
1 (4)	N/A	(0.16667,0.8333)	(0.20774,0.79226)
1, 2 (4)	(0.039156,0.73629)	(0.41667,0.91667) or (0.08333,0.58333)	(0.11187,0.56941)
1, 3 (4)	N/A	(0,1)	(0.35008,064992)
1, 2, 3 (4)	(0.38362,0.87001)	(0.083168,0.41683)	(0.23272,0.67944)
1, 2, 4 (4)	(0.35101,0.63812)	(0.041662,0.70833)	(0.22602,0.48296)

Table 2. min $[\lambda_i(W_{1\infty}^{\circ})]$ and max $[\lambda_j(W_{2\infty}^{\circ})]$

Modes	Clamped-Free Beam	Simply Supported Beam	Clamped-Clamped Beam
1 (2)	(4055.7,3.2202e-6)	(1086.8,2.915e-23)	(297.02,3.6446e-9)
1 (3)	N/A	(815.08,3.377e-7)	(294.1,3.635e-7)
1, 2 (3)	(521.7,5.506e-9)	(50.919,1.0978e-7)	(50.67,5.215e-8)
1, 3 (3)	(36.6673,1.9367e-5)	(13.4145,0)	(19.515,4.782e-7)
1, 2, 3 (3)	(106.173,0)	(13.40,0)	(9.995,0)
1 (4)	N/A	(815.08,1.0935e-6)	(294.1,1.024e-5)
1, 2 (4)	(267.95,5.3105e-6)	(50.919,4.06e-6)	(46.078,6.855e-7)
1, 3 (4)	N/A	(13.4145,0)	(19.515,4.782e-7)
1, 2, 3 (4)	(63.3421,5.0307e-9)	(6.6999,8.9684e-5)	(6.7903,1.6872e-5)
1, 2, 4 (4)	(64.0562,2.01e-10)	(3.1821,1.2292e-6)	(5.3444,1.8006e-7)

slopes at the two sensor positions is maximized for the important modes, and minimized for the unimportant modes. In the case of the clamped-free beam, it was impossible to maximize the difference in slope for the first mode while minimizing the difference in slope for the other modes. In fact, when the first mode is assumed to be the important mode, and the second and third modes were labeled unimportant, the minimum eigenvalue of the observability grammian matrix $W_{2\infty}^{\circ}$ for the unimportant modes was much greater than the maximum eigenvalue of the matrix $W_{1\infty}^{\circ}$ for the important mode. This failure illustrates the limitation in using a uniform distributed piezoelectric sensor to measure specific vibration modes.

Table 2 represents the minimum eigenvalue in subsystem 1 and the maximum eigenvalue in subsystem 2. The numbers in parentheses in the second column through the fourth column denote the minimum eigenvalue in subsystem 1 and the maximum eigenvalue in subsystem 2. As shown in Table 1, the minimum eigenvalues in subsystem 1 are maximized while the maximum eigenvalues in subsystem 2 are minimized. When the highest mode is the third mode and the important modes are the first, second, and third modes the minimum eigenvalues of $W_{1\infty}^{\circ}$ are plotted for several types of beam (Fig. 11–13). These figures illustrate the objective function $-J_0$ when the normalized locations, x_{1s}/L_b and x_{2s}/L_b, are varied from 0 to 1. The peak notes the maximum

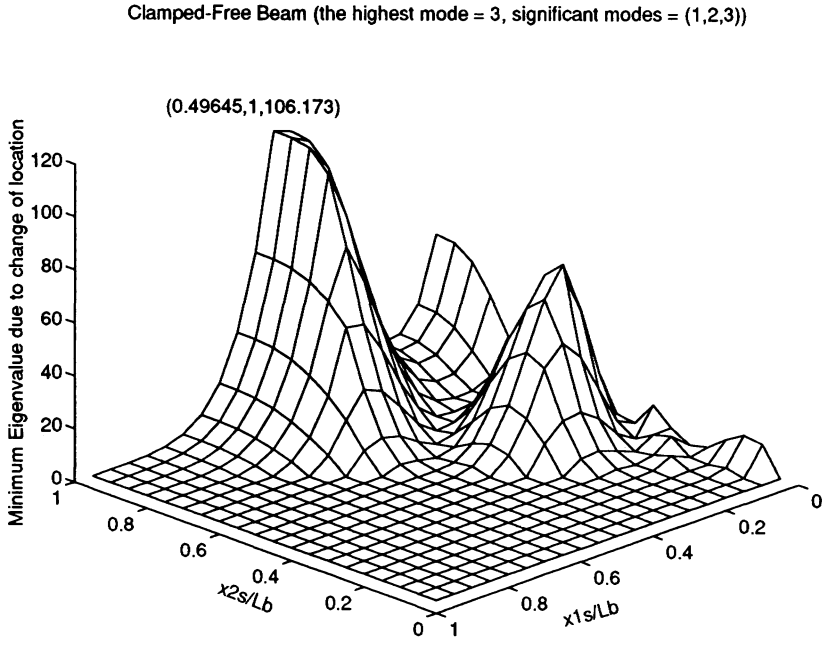

FIGURE 11 Minimum eigenvalue of W_{∞}° in clamped-free beam.

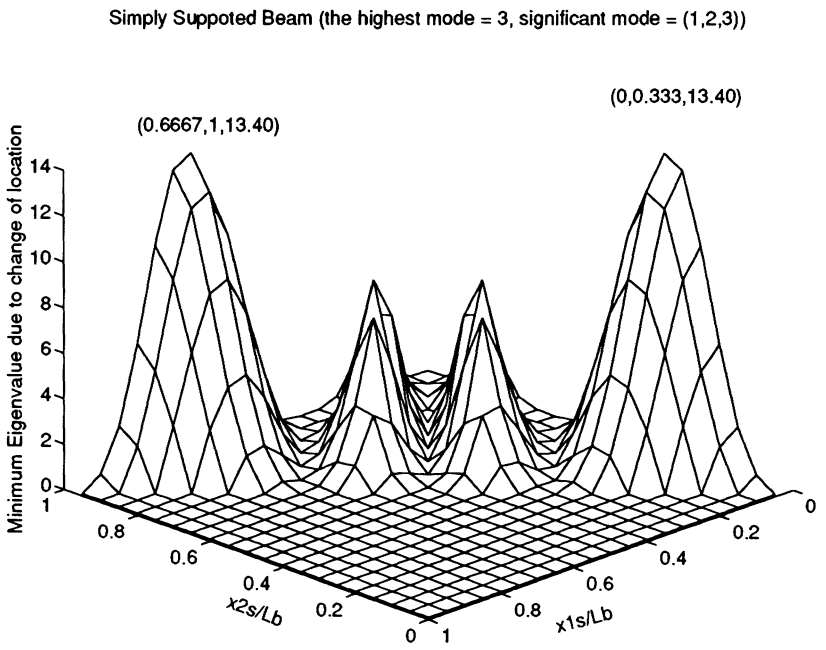

FIGURE 12 Minimum eigenvalue of W_∞^0 in simply supported beam.

value of the objective function $-J_0$ and its position indicates the optimal locations of a distributed sensor. Because x_{2s} is always greater than x_{1s}, the value of $-J_0$ is set to zero in the region that x_{2s} is less than x_{1s}. From the results, we can use the optimization criterion to find the optimal location of a uniform piezoelectric sensor to effectively sense the specific vibration modes.

OPTIMAL LOCATION OF DISTRIBUTED ACTUATOR

The optimal locations of a distributed actuator in a clamped-free, simply supported, and clamped-clamped beam are identical to those of a distributed sensor when the important modes and unimportant modes are the same for either case. The

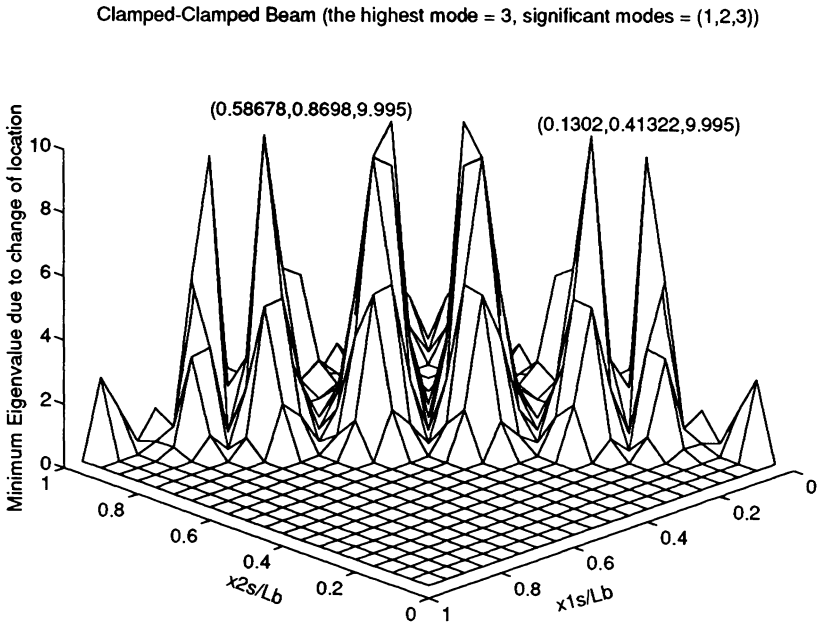

FIGURE 13 Minimum eigenvalue of W_∞^0 in clamped-clamped beam.

Table 3. min $[\lambda_i(W_{1\infty}^c)]$ and max $[\lambda_j(W_{2\infty}^c)]$

Modes	Clamped-Free Beam	Simply Supported Beam	Clamped-Clamped Beam
1 (2)	(9.048e-5,5.7137e-14)	(5.0937e-5,3.8e-32)	(5.3041e-6,4.1512e-20)
1 (3)	N/A	(3.82035e-5,3.2005e-11)	(5.252e-6,4.7105e-12)
1, 2 (3)	(2.098e-5,2.8804e-11)	(2.3866e-6,7.023e-15)	(9.0491e-7,1.3401e-12)
1, 3 (3)	(1.6712e-6,2.8667e-14)	(6.2874e-7,1.32e-28)	(3.4716e-7,8.8645e-15)
1, 2, 3 (3)	(3.3895e-6,0)	(6.2805e-7,0)	(1.7844e-7,0)
1 (4)	N/A	(3.8203-e5,8.3831e-10)	(5.252e-6,4.0569e-12)
1, 2 (4)	(1.0773e-5,1.8143e-10)	(2.3866e-6,8.3217e-15)	(8.2284e-7,1.4615e-10)
1, 3 (4)	N/A	(6.2874e-7,2.1843e-27)	(3.4716e-7,8.8645e-15)
1, 2 3 (4)	(4.078e-6,2.3138e-11)	(3.1402e-7,2.1492e-14)	1.2121e-7,1.1157e-15)
1, 2, 4 (4)	(1.145e-6,1.0609e-13)	(1.4915e-7,5.7283e-15)	(9.4257e-8,3.0269e-14)

actuator position is chosen to ensure that important modes are highly controllable, and to ensure that unimportant modes are not excited. The method through which the actuators control the modes is by exciting the slope at given points. Therefore, optimal actuator position occurs when the difference between the slopes at the two actuator positions is maximized for the important modes, and minimized for the unimportant modes. The failures for finding an optimal location of a distributed actuator in the case of the clamped-free beam is the same as the failures in the case of a distributed sensor. Table 3 represents the minimum eigenvalue in subsystem 1 and the maximum eigenvalue in subsystem 2. The numbers in parentheses in the second column through the fourth column denote the minimum eigenvalue in subsystem 1 and the maximum eigenvalue in subsystem 2. As shown in the preceding table, the minimum eigenvalues in subsystem 1 are maximized while the maximum eigenvalues in subsystem 2 are minimized. When the highest mode is the third mode and the important modes are the first, second, and third modes the minimum eigenvalues of $W_{1\infty}^c$ are plotted in the case of several types of beam (Fig. 14–16). It is interesting to note that the optimal locations of the piezoceramic actuator and the piezoelectric sensor are exactly the same when the important and unimportant modes are the same for either case. The reason is that the matrices B and C are related to the difference of the

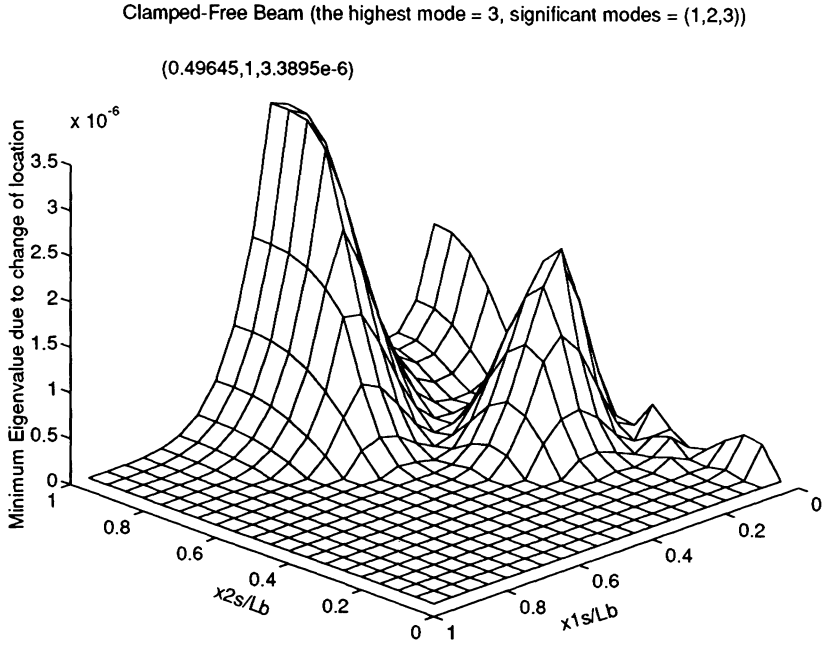

FIGURE 14 Minimum eigenvalue of W_∞^c in clamped-free beam.

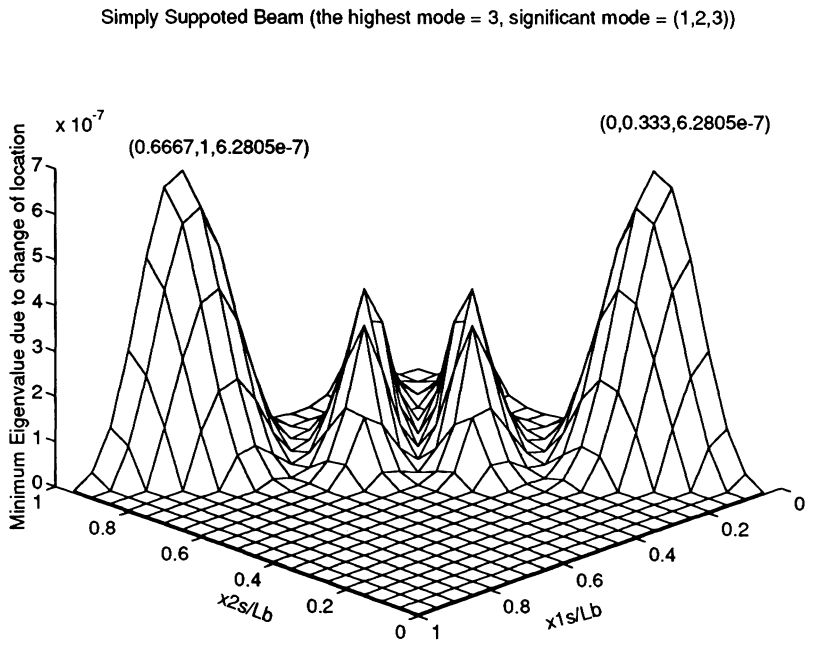

FIGURE 15 Minimum eigenvalue of W_∞^c in simply supported beam.

slopes at two end points as follows:

$$c_m = \left(\frac{d\phi_m}{dx}\bigg|_{x=x_{2s}} - \frac{d\phi_m}{dx}\bigg|_{x=x_{1s}}\right)$$

$$b_m = \left(\frac{d\phi_m}{dx}\bigg|_{x=x_{2a}} - \frac{d\phi_m}{dx}\bigg|_{x=x_{1a}}\right)$$

where the subscript m denotes the mth vibration mode. Thus it is reasonable that the optimal locations of the distributed sensor and actuator are identical. From these results, we can systematically find the optimal location of a uniform piezoelectric actuator to effectively control specific vibration modes.

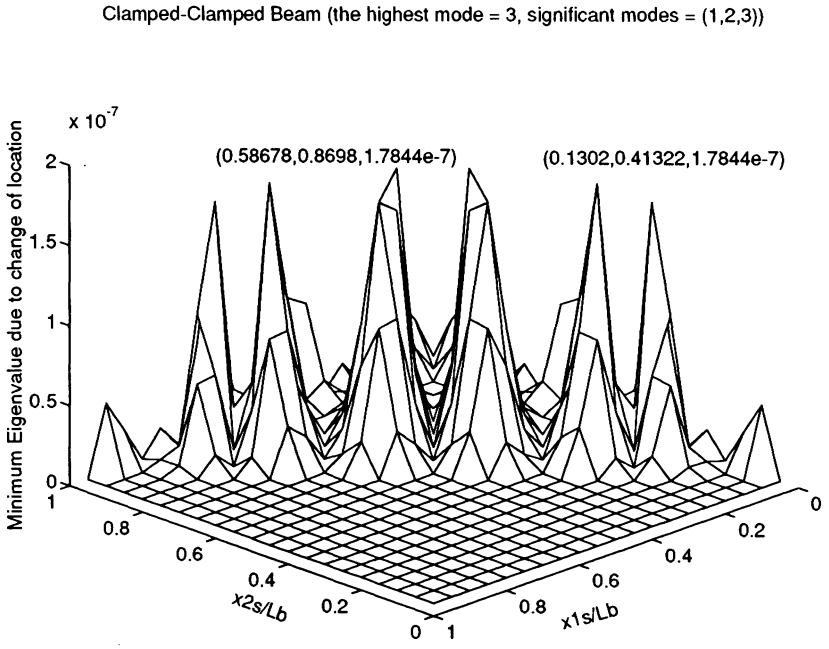

FIGURE 16 Minimum eigenvalue of W_∞^c in clamped-clamped beam.

CONCLUSION

In this article we have formulated a design method to find the optimal location of a uniform distributed sensor/actuator pair for a beam with several types of boundary conditions. The observability grammian matrix was chosen to provide a performance index for the optimal location of distributed sensors and the controllability grammian matrix was chosen to provide a performance index for the optimal location of distributed actuators. From the examples, we can see that using the minimum eigenvalues of the observability/controllability grammian matrices as performance indices is appropriate for determining the optimal location of a distributed sensor/actuator pair. The optimal locations of distributed sensor/actuator pairs are identical in the case of a beam when the important and unimportant vibration modes are the same for both the sensor and actuator.

REFERENCES

Arbel, Ami, 1981, "Controllability Measures and Actuator Placement in Oscillatory Systems," *International Journal of Control,* Vol. 33, pp. 565–574.

Bailey and Hubbard, 1987, "Nonlinear Control of a Distributed System: Simulation and Experimental Results," *Transactions of ASME Journal of Dynamic Systems, Measurement, and Control,* Vol. 109, pp. 133–139.

Crawley E. F., and de Luis, J., 1986, "Experimental Verification of Distributed Piezoelectric Actuators for Use in Precision Space Structures," *AIAA Paper,* 86-0878, pp. 116–124.

Hamden, A. M., and Nayfeh, A. H., 1989, "Measures of Modal Controllability and Observability for First- and Second-Order Linear Systems," *Journal of Guidance,* Vol. 12, pp. 421–428.

Institute of Electrical and Electronics Engineers, Inc., 1987, "IEEE Standard on Piezoelectricity," *ANSI/IEEE Std.* 176-1987.

Lee, C. K., and Moon, F. C., 1990, "Modal Sensors/Actuators," *Transaction of ASME Journal of Applied Mechanics,* Vol. 57, pp. 434–441.

Lee, C. K., Chiang, W. W., and O'Sullivan, T. C., 1991, "Piezoelectric Modal Sensor/Actuator Pairs for Critical Active Damping Vibration Control," *Journal of the Acoustical Society of America,* Vol. 90, pp. 374–384.

Lim, K. B., 1992, "Method for Optimal Actuator and Sensor Placement for Large Flexible Structures," *Journal of Guidance,* Vol. 15, pp. 49–57.

Maghami, P. G., and Joshi, S. M., 1993, "Sensor-Actuator Placement for Flexible Structures With Actuator Dynamics," *Journal of Guidance, Control and Dynamics,* Vol. 16, pp. 301–307.

The MathWorks Inc., 1991, "PRO-Matlab User's Manual."

Sessler, G. M., 1981, "Piezoelectricity in Polyvinylidenefluoride," *Journal of the Acoustical Society of America.,* 70, pp. 1596–1608.